Paper
Int'l J. of Aeronautical & Space Sci. 17(2), 222–231 (2016)
DOI: http://dx.doi.org/10.5139/IJASS.2016.17.2.222

IJASS
International Journal of Aeronautical and Space Sciences

An Efficient Attitude Reference System Design Using Velocity Differential Vectors under Weak Acceleration Dynamics

Byungjin Lee* and Sukchang Yun**

Department of Aerospace Information Engineering, Konkuk University, 120 Neungdong-ro, Gwangjin-gu, Seoul 05029, Republic of Korea

Hyung-Keun Lee***

Korea Aerospace University, 34-45, Hanggongdaehak-ro, Deogyang-gu, Goyang-si, Gyeonggi-do 10540, Republic of Korea

Young Jae Lee** and Sangkyung Sung*******

Department of Aerospace Information Engineering, Konkuk University, 120 Neungdong-ro, Gwangjin-gu, Seoul 05029, Republic of Korea

Abstract

This paper proposes a new method achieving computationally efficient attitude reference system for low cost strapdown sensors and microprocessor platform. The main idea in this method is to define and compare velocity differential vectors, geometrically computed from INS and GPS data with different update rate, for generating attitude error measurements which is further used for filter construction. A quaternion based Kalman filter configuration is applied for the attitude estimation with the adapted measurement model of differential vector comparison. Linearized model for Extended Kalman Filter and low pass filtered characteristics of measurement greatly extend the affordability of the proposed algorithm to the field of simple low cost embedded systems. For performance verification, experiment are done employing a practical low cost MEMS IMU and GPS receiver specification. Performance comparison with a high grade navigation system demonstrated good estimation result.

Key words: attitude reference system, velocity differential, quaternion, Kalman filter, low cost MEMS, IMU.

1. Introduction

Unmanned vehicles have been widely designed and developed for various ground and airborne applications with three dimensional dynamical motions from smart cruise, sky overlook surveilence, product delivery, target surface or space monitoring, robotics education to personal entertainment system. Essential technology for the unmanned system as well as the UAV includes attitude determination for manual or assisted guidance and control. When cost or weight makes issues, precise navigation system considering even the Schuler effect due to an on-flat rotating Earth or implementing very complicated filters containing higher order error dynamics are not acceptable. Instead, a low-cost attitude and heading reference systems that just depends on the light and cheap strapdown inertial sensors can be a good alternative.

ARS(Attitude Reference System) is both simple and popular system that can measure an attitude in various applications [1-2]. The essential feature of ARS is the integration between the integral result of angular velocity from gyroscopes and the gravity vector direction from accelerometers. This is because gyroscope measuring the angular velocity can be applied to high angular dynamic environments while the gravity vector, measured by accelerometer, computes directly the horizontal direction attitude, i.e., roll and pitch. The integration of

* Graduate Student
** Graduate Student
*** Professor
**** Professor
***** Professor, Corresponding Author: sksung@konkuk.ac.kr

Received: March 9, 2015 Revised: January 16, 2016 Accepted: January 21, 2016

http://ijass.org pISSN: 2093-274x eISSN: 2093-2480

gyroscope and accelerometer generally supplements accuracy and sensitivity to some extents [3].

However considering a low cost sensor platform even with installation error, a simple ARS integration may yield a significant performance degradation. Estimating the vehicle's attitude by simply integrating the rigid body kinematic equation of rotation and using the angular rate from gyroscopes is not safe in long-term applications. Specifically, the random bias error behaves as a principal factor for attitude divergence. To correct this, the gravity vector measured by accelerometer can be used, which is free from a divergence property [3-5]. Yet during a translational motion, the accelerometer measures specific force (gravity and dynamic forces) simultaneously, thus it may be hard to estimate true roll and pitch orientation through rate integration of acceleration measurements.

There are various research results that have resolved these traditional ARS problems by integrating heterogeneous sensor measurements such as magnetometer, vision sensor and GPS [6-8]. In case of magnetometer application, the reference attitude direction could be effectively augmented via the earth magnetic information. However due to the environmental noise factors, the local magnetic field is subject to distortion in measurement. Vision sensor can also generate relative navigation fix information that is robust to inertial perturbations, yet its implementation requires heavy computational burdens for achieving accuracy and sufficient update rate. Besides navigation data greatly relies on the visual environment, thus it suffers from filtering continuity under a general case. In GPS integration case, a simple strategy is to extract the additive dynamic force term from the accelerometer measurement with the help of GPS velocity differential [8]. Thus gravity term can be successfully extracted from the strapdown measurement of accelerometer. In practice, extracting dynamic acceleration is not sufficiently fast for computational integrity when a middle or low cost GPS receivers are used. Comparatively, a full INS/GPS integrated navigation with error state model can be an extravagant implementation necessitating improper processing capacity. Although a typical INS/GPS integration filter can generate full inertial solution and attitude correction accurately, the convergence speed of attitude can be slower than that of the direct numerical computation method. Moreover, if the divergence speed of the attitude by the angular velocity integration is faster than the filter convergence speed, the attitude correction cannot be acheived, which frequently occurs for the applications using low cost IMUs [9-10].

Considering these characteristics and drawbacks from the reported ARS studies, this paper newly suggests an efficient method to compute the local horizontal attitude of a dynamic vehicle. The proposed algorithm fundamentally succedes a traditional ARS configuration, which combines IMU measurement with GPS velocity measurements. With the assumption of 'weak acceleration' widely adopted in VTOL UAV or land vehicle applications [3-4,19-21], the proposed algorithm uniquely combines each velocity differential vectors in the measurement formulation, which will consequently achieve both computational efficiency and estimation performance. Specifically, the designed configuration takes advantage of the quarternion measurement using a low cost GPS receiver with a slow update rate (2sec). As the presented method inherits robustness to vibration through the proposed error model, a raw data processing such as low pass filter is unnecessary. Besides, this method generates directly the filter measurement in a quarternion form, the correction is fast and the high order matrix computation is not needed. With these advantages, it is possible to employ low cost IMU and low speed microprocessors for implementing the algorithm.

The proposed algorithm is evaluated through hardware testbed equiped with a low cost MEMS IMU and a GPS receiver. And for verifying the performance, the test result was compared with the result obtained from the post processing of the commercial INS/GPS integration system containing a tactical grade IMU and a high performance GPS receiver supported by the RTK.

2. Algorhtim Formulation

2.1 Gyro Error and Velocity Differential Model

Considering a simple error model, the measurement equation of rate gyroscope can be represented by an additive equation of true angular rate with white gaussian and bias noises.

$$\vec{\omega} = \vec{\omega}_{true} + \vec{b}_g + \vec{n}_g \tag{1}$$

In (1), $\vec{\omega}$ is output of the rate gyroscope. $\vec{\omega}_{true}$ is a true angular rate of strapdown system. $\vec{n}_g$ and $\vec{b}_g$ are a white noise and bias error term, respectively. In this model, the typical error source like angular random walk is not employed since the resulting attitude error is negligible due to its white noise property. By integrating $\vec{\omega}$ within a certain time interval, the attitude vector is calculated as follows

$$\vec{\Phi} = \vec{\Phi}_{true} + \int_t^{t+\Delta t} \vec{n}_g \, dt + \int_t^{t+\Delta t} \vec{b}_g \, dt \tag{2}$$

Considering the white noise characteristics $\vec{n}_g$, integral output during a certain time period can be rearranged into the following equation,

$$\vec{\Phi} \approx \vec{\Phi}_{true} + \vec{b}_g \cdot \Delta t \tag{3}$$

Owing to the non-zero mean and colored noise property of the bias term, attitude determination through simple integration greatly suffers from inaccuracy especially in a low grade sensor platfrom, even with short integration period.

The accelerometer in the traditional ARS typically measures the earth gravity vector to calculate the roll and pitch angle. But the onboard accelerometer measures the gravity and dynamic accelerations collectively during a vibratory or translational motion, which results in critical error factors in the ARS computation. Thus, an effective attitude error model that compares two velocity differential vectors (ΔVs) reflecting both gravity and dynamic acceleration effect needs to be devised. Specifically, one of the velocity differential vectors is obtained through GPS velocity with gravity updates and inertial velocity through an integration of accelerometer output in the body frame.

Let us derive each velocity diffrential term. Eq. (4) describes the total accelerometer output in the body frame.

$$\vec{A}_{body} = \vec{g}_{body} + \vec{a}_{body} + \vec{b}_a + \vec{n}_a \tag{4}$$

where $\vec{g}$ is the gravity acceleration, $\vec{a}$ is the dynamic acceleration, $\vec{n}_a$ is the white noise, $\vec{b}_a$ is bias. Next, Eq. (5) derives the velocity differenitial vector in the local NED coordinate during a fixed integral period.

$$\Delta\vec{V}_{INS,NED} = \int_t^{t+\Delta t} \boldsymbol{C}_B^N(\vec{\Phi}) \cdot \vec{A}_{body}\, dt \tag{5}$$

$\vec{\Phi}$ denotes a pre-computed attitude at the integraion instance, which is used in computing the direction cosine matrix $\boldsymbol{C}_B^N(\vec{\Phi})$ from body frame to navigation frame (NED frame). Then (5) is rearranged as

$$\Delta\vec{V}_{INS,NED} = \int_t^{t+\Delta t} \boldsymbol{C}_B^N(\vec{\Phi}) \cdot (\vec{g}_{body} + \vec{a}_{body})\, dt + \int_t^{t+\Delta t} \vec{b}_a dt + \int_t^{t+\Delta t} \vec{n}_a dt \tag{6}$$

By considering a proper integration interval and relative magnitude, it is assumed that the white noise and bias term of accelerometer output can be effectively eliminated during integration, which then calculates the approximated velocity differential vector as shown in (7). Deciding integration interval relies on each sensor's performance specification and application, yet it can be simply set as a typical GPS update rate (0.5Hz) during which hundreds of intermediate IMU data are accumulated.

$$\Delta\vec{V}_{INS,NED} \approx \int_t^{t+\Delta t} \boldsymbol{C}_B^N(\vec{\Phi}) \cdot \vec{g}_{body}\, dt + \int_t^{t+\Delta t} \boldsymbol{C}_B^N(\vec{\Phi}) \cdot \vec{a}_{body}\, dt \tag{7}$$

In (7), $\vec{\Phi}$ is computed by adding $\vec{\Phi}_{True}$ and the accumulated bias error in (3). Note that, without sensor output error, $\boldsymbol{C}_B^N(\vec{\Phi}) \cdot \vec{g}_{Body}$ reduces $\vec{g}_{NED} = [0, 0, \text{-g}]$. Similarly, $\boldsymbol{C}_B^N(\vec{\Phi}) \cdot \vec{a}_{body}$ describes the gravity-free acceleration in the NED frame ($\vec{a}_{NED}$) at the zero error condition. Note that $\Delta\vec{V}_{INS,NED}$ virtually combines a pure dynamic term $\vec{a}$ and a time invariant constant term $\vec{g}$ from the gravity. Therefore, assuming no accumulation error from the gyro measurement, the pure dynamic term in (7) is equivalent to the GPS and gravity combined velocity increment in the NED frame, $\Delta\vec{V}_{GPS,NED}$.

It is remarkable that while most conventional approaches calculate velocity through accelerometer measurment by removing the gravity vector, yet the proposed algorithm uses a total velocity increment containing both gravity and dynamic force term described in (7). In this scheme, the vector deviation of inertial velocity differential from a reference differential vector, i.e., $\Delta\vec{V}_{GPS,NED}$, is employed to further formulate the measurement model of the proposed attitude estimation.

2.2 Model Formulation via Velocity Increment Vector

To formulate measurement model, a reference velocity increment vector is defined, which is a combined vector of a GPS velocity differential ($\Delta\vec{V}_{GPS,NED}$) with a local vertical gravity ($\vec{g}_{NED} \cdot \Delta t$). In Fig. 1, the reference vector is represented by $\Delta\vec{V}_{Ref,NED}$. Then it is observed the velocity increment $\Delta\vec{V}_{INS,NED}$ presents a varional error from the reference vector due to the sensor's inherent error terms. In

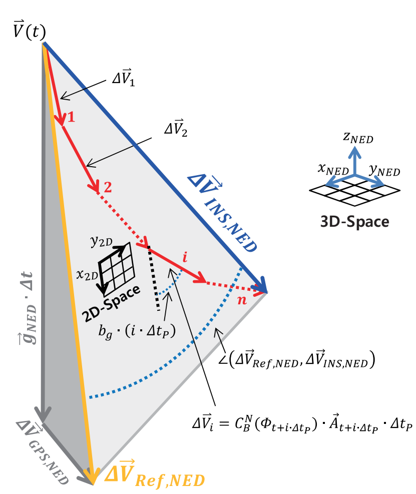

Fig. 1. The relation between $\Delta\vec{V}_{Ref,NED}$ and $\Delta\vec{V}_{INS,NED}$ through gyro bias

DOI: http://dx.doi.org/10.5139/IJASS.2016.17.2.222

Fig. 1, Δt_P is the update period of the inertial sensors, which is usually set to 0.01sec in experiment. n is the number of the IMU propagation during the GPS update period, thus $n \cdot \Delta t_P$ equals the GPS update period (Δt, 2sec). Assuming $\vec{b}_g$ maintains slowly-varying error dynamics during Δt, each term in $\boldsymbol{C}_B^N(\vec{\Phi}_{t+i\cdot\Delta t_P}) \cdot \vec{A}_{t+i\cdot\Delta t_P} \cdot \Delta t_P$ can be located in the plane defined by velocity differential vectors ($\Delta\vec{V}_{INS,NED}$ and $\Delta\vec{V}_{Ref,NED}$), since the same error vector propagations are accumulated with '$\vec{g} \gg \vec{a}$' condition.

For a simple illustration, consider the plane of interest on which $\Delta\vec{V}_{INS,NED}$ and $\Delta\vec{V}_{Ref,NED}$ are located, as shown in 2D-Space coordinate in Fig. 1. '2D-Space' in Fig. 2 is a temporary frame for the attitude error model by gyroscope bias. The x-axis in this frame has same direction with $\Delta\vec{V}_{Ref}$. And $\Delta\vec{V}_{Ref}$, $\Delta\vec{V}_{INS}$ and all vectors of the accelerometer could be placed on the same plane during Δt. Fig. 2 draws the local 2D coordinate plane. In the figure, $\Delta\vec{V}_{Ref,NED}$ is rotated to a vertical vector, $\Delta\vec{V}_{Ref,2D}$. Then $\Delta\vec{V}_{INS,2D}$ is the numerical integration result of the acceleration vector denoted by $\vec{A}_{2D}$ as expressed in (8).

$$\Delta\vec{V}_{INS,2D} = \sum_{i=1}^{n}\left(\left|\vec{A}_{2D}(t + i \cdot \Delta t_P)\right| \cdot \vec{S}_i \cdot \Delta t_P\right) \tag{8}$$

$$\text{where } \vec{S}_i = \begin{bmatrix} cos\left(\varepsilon_g \cdot (i \cdot \Delta t_P)\right) \\ sin\left(\varepsilon_g \cdot (i \cdot \Delta t_P)\right) \end{bmatrix}.$$

Note that $\vec{A}_{2D}$ consists of the earth gravity and the dynamic acceleration. Also, the projected gyro bias term is denoted by $\varepsilon_g = k|\vec{b}_g|, 0 < k \leq 1$.

Now assuming a weak acceleration condition and whiteness of acceleration noise, the gravity serves as dominant factor and $\vec{A}_{2D}$ can be factored out as below

$$\Delta\vec{V}_{INS,2D} \cong \left|\vec{A}_{2D}\right| \cdot \Delta t_P \cdot \textstyle\sum_{i=1}^{n}(\vec{S}_i) \tag{9}$$

Even though bias term in gyro mainly causes attitude divergence, each update in bias error $\vec{b}_g(i \cdot \Delta t_P)$ is very small during a short time period. Thus velocity differential vector in the 2D-projection plane is re-arranged into

$$\begin{aligned} \Delta\vec{V}_{INS,2D} &\cong \left|\vec{A}_{2D}\right| \cdot \Delta t_P \cdot \sum_{i=1}^{n}\left(\vec{S}_i{}'\right) \\ &= \left|\vec{A}_{2D}\right| \cdot \Delta t_P \cdot \begin{bmatrix} n \\ \varepsilon_g \cdot \Delta t_P \cdot \dfrac{n\cdot(n+1)}{2} \end{bmatrix} \end{aligned} \tag{10}$$

since the trigonometric vector is simplified into

$$\vec{S}_i \cong \vec{S}_i{}' = \begin{bmatrix} 1 \\ \varepsilon_g(i \cdot \Delta t_P) \end{bmatrix}$$

The main idea of the proposed method is to estimate attitude error between velocity differental vectors in the projection plane, which is illustrated in Fig. 2. In the filter configuration, the error equation is formulated through the inner angle (∠) between $\Delta\vec{V}_{Ref,2D}$ and $\Delta\vec{V}_{INS,2D}$. Again considering small bias error update condition,

$$\begin{aligned} &\angle\left(\Delta\vec{V}_{Ref,2D}, \Delta\vec{V}_{INS,2D}\right) \\ &\quad\cong \tan^{-1}\left(\frac{\varepsilon_g \cdot \Delta t_P \cdot \dfrac{n\cdot(n+1)}{2}}{n}\right) \\ &\quad\cong \varepsilon_g \cdot \Delta t_P \cdot \frac{n+1}{2} \end{aligned} \tag{11}$$

Practically, Δt_P is much shorter than Δt. Therefore the number of the updated IMU data during a GPS update time (i.e., n) is very large. Thus (11) is simplfied into (12).

$$\angle\left(\Delta\vec{V}_{Ref,2D}, \Delta\vec{V}_{INS,2D}\right) \cong \tfrac{\varepsilon_g \cdot \Delta t}{2} \tag{12}$$

At (12), note that the inner angle between $\Delta\vec{V}_{Ref,2D}$ and $\Delta\vec{V}_{INS,2D}$ is described through gyro bias and Δt. It is notable that the right hand side of (12) is equal to the half of the bias increase during transition time, i.e., $\Phi_\varepsilon \coloneqq \varepsilon_g \cdot \Delta t$. Since the attitude error is preserved through a rotational transformation, the inner angle of $\Delta\vec{V}_{Ref,NED}$ and $\Delta\vec{V}_{INS,NED}$ is computed in the same way. Consequently, the above equation can be rearranged into

$$\angle\left(\Delta\vec{V}_{Ref,NED}, \Delta\vec{V}_{INS,NED}\right) = \Phi_\varepsilon/2 \tag{13}$$

For deriving a measurement model, a quarternion based attitude estimation method is adapted. Quaternion is a popular mathematical tool that can easily manipulate attitude computation in 3 dimensional coordinate system. Parameters in quaternion represent a scalar deciding rotation quantity and vector elements deciding rotation orientation. Eq. (14) describes the basic form of quaternion.

$$\boldsymbol{q}_\varepsilon = \begin{bmatrix} cos\dfrac{\Phi_\varepsilon}{2} & sin\dfrac{\Phi_\varepsilon}{2} \cdot [\alpha \quad \beta \quad \gamma] \end{bmatrix}_{4\times1}^{T} \tag{14}$$

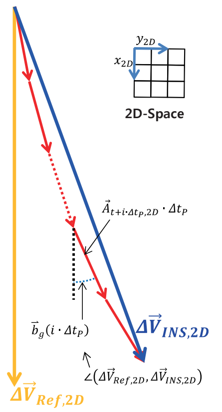

Fig. 2. The 2D-projection plane for analyzing error accumulation.

In (14), Φ_ε represents a rotation angle, and the nomalized vector $[\alpha \ \ \beta \ \ \gamma]^T$ represents the rotation axis. Observing the vector product properties and error equation, attitude error in quaternion form can be drawn using the velocity measurements from different sensors. For the ease of equation development, body frame is taken as below.

$$\boldsymbol{q}_\varepsilon = \begin{bmatrix} (\Delta\vec{V}_{INS,body})_n \cdot (\Delta\vec{V}_{Ref,body})_n \\ (\Delta\vec{V}_{INS,body})_n \times (\Delta\vec{V}_{Ref,body})_n \end{bmatrix} \tag{15}$$

where

$$\begin{aligned} \Delta\vec{V}_{INS,body} &= \boldsymbol{C}_N^B(\vec{\Phi}) \cdot \Delta\vec{V}_{INS,NED} \\ \Delta\vec{V}_{Ref,body} &= \boldsymbol{C}_N^B(\vec{\Phi}) \cdot \Delta\vec{V}_{Ref,NED} \end{aligned} \tag{16}$$

$(\ )_n$: normalization of the vector in bracket

2.3 Integration Filter

Since MEMS IMU in a strapdown platfrom is considered, the angular rate is denoted as $\vec{\omega}_b$ or $(p,\ q,\ r)$ in a body frame. Quaternion differentiation is used for the attitude propagation as shown in (17). [12-13,22]

$$\boldsymbol{q}_k^- = \boldsymbol{q}_{k-1} * f_{eulr2qua}(\vec{\omega}_b \cdot \Delta t_P) \tag{17}$$

where $f_{eulr2qua}(\cdot)$ represents convertion function from the Euler angle to quaternion variables and '*' denotes quaternion multiplication, and $\vec{\omega}_b = [p \ \ q \ \ r]^T$. In (17), q_k is a quarternion representation at epoch k, and superscript '-' implies a priori process before measurment. The Euler integration method can be used for computing the attitude propagation via a quternion characteristic. [14]

To linierize (17), quaternion differentiation is used. Eq. (18) represents the linierazed propagation equation.

$$\begin{aligned} \boldsymbol{q}_k^- &= \boldsymbol{q}_{k-1} + \delta\boldsymbol{q}_k^- \\ &\cong \boldsymbol{q}_{k-1} + \frac{\partial \boldsymbol{q}_{k-1}}{\partial t} \cdot \Delta t_p \end{aligned} \tag{18}$$

where

$$\frac{\partial \boldsymbol{q}_{k-1}}{\partial t} = \frac{1}{2} \cdot \begin{bmatrix} -q_1 \cdot p - q_2 \cdot q - q_3 \cdot r \\ q_0 \cdot p + q_2 \cdot r - q_3 \cdot q \\ q_0 \cdot q - q_1 \cdot r + q_3 \cdot p \\ q_0 \cdot r + q_1 \cdot q - q_2 \cdot p \end{bmatrix}$$

In (18), q_0~q_3 represents each element of quaternion For constructing process model of error dynamics, state is newly defined by $\delta q_k = q_k - q_{k-1}$. Here δq_k is further linearized using (18).

$$\begin{aligned} \delta\boldsymbol{q}_k^- &\cong \frac{\partial \boldsymbol{q}_k^-}{\partial t} \cdot \Delta t_p \\ &= \left(\frac{\partial \boldsymbol{q}_k^-}{\partial \boldsymbol{q}_{k-1}} \cdot \frac{\partial \boldsymbol{q}_{k-1}}{\partial t} + \frac{\partial \boldsymbol{q}_k^-}{\partial \vec{\omega}_b} \cdot \frac{\partial \vec{\omega}_b}{\partial t} \right) \cdot \Delta t_p \\ &= \boldsymbol{A}_q \cdot \delta\boldsymbol{q}_{k-1} + \boldsymbol{B}_q \cdot \delta\vec{\omega}_b \end{aligned} \tag{19}$$

where

$$\boldsymbol{A}_q = I_{4\times4} + \frac{1}{2} \cdot \begin{bmatrix} 0 & -p & -q & -r \\ p & 0 & r & -q \\ q & -r & 0 & p \\ r & q & -p & 0 \end{bmatrix} \cdot \Delta t_P$$

$$\boldsymbol{B}_q = \frac{1}{2} \cdot \begin{bmatrix} -q_1 & -q_2 & -q_3 \\ q_0 & -q_3 & q_2 \\ q_3 & q_0 & -q_1 \\ -q_2 & q_1 & q_0 \end{bmatrix} \cdot \Delta t_P$$

It is straightforward to derive error covariance matrix (P) of the Kalman filter through error residual.[15-16] The time propagation for covariance matrix is given by (20), where Q typically relies on the performance of gyroscope. In practice, a 3×3 tuning matrix η_Q is employed for filter implementation, as shown in (21).

$$P_{q,k}^- = \boldsymbol{A}_q \cdot \boldsymbol{P}_{q,k-1} \cdot \boldsymbol{A}_q^T + \boldsymbol{B}_q \cdot \boldsymbol{Q} \cdot \boldsymbol{B}_q^T \tag{20}$$

$$\boldsymbol{Q} = \begin{bmatrix} var(p) & 0 & 0 \\ 0 & var(q) & 0 \\ 0 & 0 & var(r) \end{bmatrix} + \eta_Q \tag{21}$$

From (15), the measurement model takes advantage of a quaternion formulation with the observation matrix (H_q) given as $I_{4\times4}$ [17]. Thus

Note that q_ε represents a geometric residual, thus it cannot be used for computing residual directly. In quaternion domain, a virtual measurement (z_k) is derived via the quarterion multiplication of a priori estimate (q_k^-) and the geometric residual (q_ε).

Covariance update and calculating Kalman gain follows the general EKF (extended Kalman filter) framework in Eq. (23) and (24). Here, R_q represents measurement noise, which is related with the performance of the used accelerometer and GPS. Similarly, a tuning facor is considered for improving estimation performance. Eq. (25) represents a simple tuning parameter η_o.

$$\begin{aligned} \boldsymbol{q}_k &= \boldsymbol{q}_k^- - \boldsymbol{K}_{q,k} \cdot (\boldsymbol{z}_k - \boldsymbol{q}_k^-) \\ \boldsymbol{z}_k &= \boldsymbol{q}_k^- * \boldsymbol{q}_\varepsilon \end{aligned} \tag{22}$$

$$\begin{aligned} \boldsymbol{K}_{q,k} = \boldsymbol{P}_{q,k}^- \cdot \boldsymbol{H}_q^T \\ \cdot \left(\boldsymbol{H}_q \cdot \boldsymbol{P}_{q,k}^- \cdot \boldsymbol{H}_q^T + \boldsymbol{R}_q \right)^{-1} \end{aligned} \tag{23}$$

$$\boldsymbol{P}_{q,k} = \boldsymbol{P}_{q,k}^- - \boldsymbol{K}_{q,k} \cdot \boldsymbol{H}_q \cdot \boldsymbol{P}_{q,k}^- \tag{24}$$

$$\boldsymbol{R}_q = \eta_o \cdot \boldsymbol{I}_{4\times4} \tag{25}$$

Practically, time propagation period is the same as the IMU update rate (Δt_P=0.01sec). On contrast, the correction using measurement (q_e) operates in every GPS update period (Δt=2sec).

3. Algorithm Characteristics And Implementation

The proposed attitude estimation has an advantage of computational efficiency. Principally it adopts a quarternion based ARS scheme, which incorporates efficient numerical operations like vector product and numerical integration for generating pre-filter information. Also using a geometrically driven measurement q_k, filter structure is relatively simple than other works [13, 17]. Similar with a loosely coupled INS/GPS integration, filter update period are governed by the GPS periods, usually Δt=2sec, which allows an efective implementation through a microprocessor capacity.

Assumptions and consraints are notable in the algorithm. First, as previously mentioned, a 'weak acceleration' condition is basically assumed. That implies '$\vec{g} \gg \vec{a}$', but the assumption is obviously different from the previous methods because of the error model (8~15). But in (9~10), weak acceleration' assumption is used for deriving the error model. So if $\vec{a}$ is too dynamically changed, these two equations could have a model error. So, even though the proposed algorithm can be applied to a high dynamic maneuvering case, yet it will cause an increased attitude estimate error. But it affects the error much smaller compar ing with the previous methods. Second, the acceleration magnitude is assumed to be constant during measurement update period. Through this assumption, attitude error, $\Delta\vec{V}_{INS,2D}$ in (9) is successfully obtained from (8). Note that a virtual gravity factor can be devised to compensate for the error increase during attitude determination. This factor can amplify the earth gravity bigger than g. Assuming a bigger g, $\Delta\vec{V}$ vectors become larger, thus the condition of '$\vec{g} \gg \vec{a}$' gets stronger. The detailed implementation about the virtual gravity is out of scope of this paper. And third, IMU and GPS receiver are placed at center of mass of the platform.

Computational requirement for algorithm includes a much faster IMU rate Δt_p over a GPS update rate Δt. Presently, most IMU provides data rate up to 100Hz with a fast microprocessor capacity, thus can satisfy the approximation in (12) with the GPS update in 2 sec.

Typically, the measurment update period depends on the GPS update rate. A sufficiently long update period is required since the white noise and random vibration effect can be effecitvely mitigated through the integration operation during Δt. On the other hand, a long measurment update period yields sparse attitude estimate results, which may result in a large attitude error. A sparse measurement update may cause a discrete 'step effect.' In the algorithm, the step effect is minimized by introducing a multiple sequential computational windows even with the same measurment update period Δt. The number of multiple windows within Δt is determined by the maximum of GPS receiver update time.

Figure 3 shows the step effect reduction by applying multiple computation windows. With a conventional GPS receiver with 5Hz output rate, measurement update can be virtually provided in every 200 msec using the same algorithm structure proposed. Note that for each update period of 200 msec, GPS velocity is stored and manipulated to compute $\Delta\vec{V}_{GPS,NED}$ using the GPS velocity 2 sec earlier. In the figure, it can be easily observed the more frequent measurement update outcomes a reduced step effect. Thus, the presented method accomplished a more frequent update rate of 5 Hz with the large computation window condition of n = 200. Fig. 4 shows the estimation precision enhancement with the help of the step effect reduction method.

4. Experiment And Discussion

For demonstrating the estimation performance of the proposed algorithm, navigation experiment using a ground vehicle platform is done. Sensor modules onboard the test

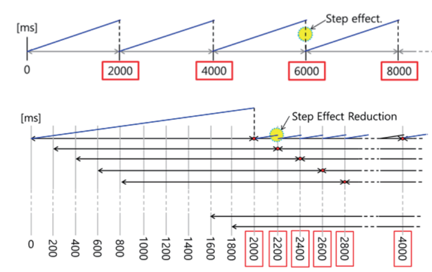

Fig. 3. Step effect and multiple sequential update windows reducing step effects

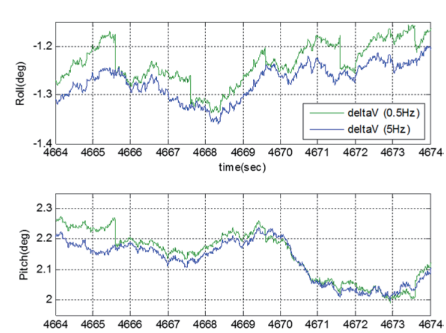

Fig. 4. Attitude estimation results before step reduction (upper) and after step reduction (lower)

vehicle and horizontal trajectory are shown in Fig. 5.

Specification of the sensor used for the experiment is shown in Table 1.

The GPS receiver of the reference devices was installed with another GPS receiver of a ground station. The ground station was located at the center of the experiment place for GPS RTK. The GPS receiver provides both the code data and L1, L2 carrier data for RTK result [18]. The outputs of the IMU and GPS of the reference devices were treated by a commercial program (Inertial Explore®) to get the exact position, velocity and attitude information. ADIS 16407 is a 10 DoF sensor with a 3 axis gyroscope, accelerometer, magnetometer and a barometer. During experiment, outputs from gyroscope and accelerometer are stored, synchronously with GPS SBAS data, and post-processed using the proposed algorithm.

The initial attitude of roll and pitch are determined during the initial static period of 10 seconds, which are computed from the gravity vector via the accelerometer. Also the gyroscope bias is set to the averaged output during the static periods. Focused on the horizontal attitude, initial yaw angle is set to the heading of reference devices. All attitude is calculated in quaternion, and it is converted to Euler angle to make the result figures.

Using the acquired data, the reference ARS with GPS compensation is analyzed first [23]. The measured specific force by accelerometer is compensated with the differential result of GPS velocity (dotVGPS). Because of 5Hz GPS update rate, the differential result is also 5Hz and very rough. So the

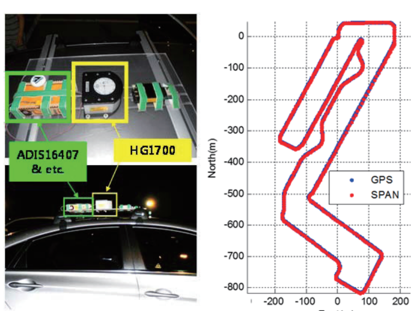

Fig. 5. Sensor modules onboard vehicle and test trajectory (drawn by reference GPS system)

Table 1. The experiment component

Date	2013/06/15(yyyy/mm/dd) 11:30 PM.
Place	37.291423, 127.209383(Lat, Lon), radius 500m area
Reference devices	NovAtel SPAN - IMU: Honeywell HG1700-AG58 - GPS: NovAtel Propak-V3 - NovAtel Inertial Explore® Post Processing
Used devices	IMU: Analog Devices ADIS 16407 (100Hz) GPS: NovAtel OEMV-1 (5Hz)

measurement results with 100Hz accelerometer have high noise and error. To mitigate excessive measurement noise, the average value of accelerometer is used. In this process, accelerometer update rate can be reduced from 100 to 5Hz. In Fig. 6, these results are shown.

In the figure, the 5Hz average result has less noise, but

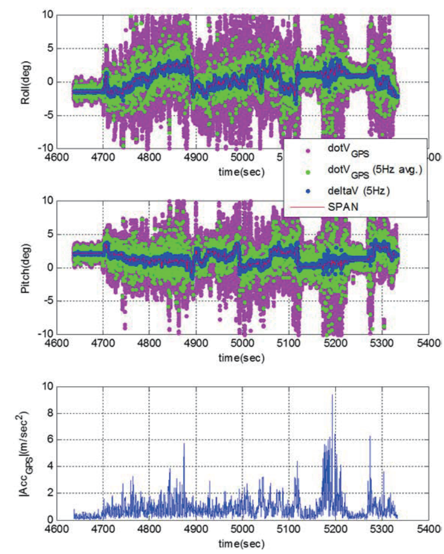

Fig. 6. The ΔVs Measurement result comparing with the reference ARS method

Table 2. The standard derivation of roll error [˚] according to the added gyroscope bias

(Upper row of each pair: $dotV_{GPS}$(5Hz avg.); lower row: *deltaV(5hz)*)

Bias Error in Y-Axis		Bias Error in X-Axis: $-10e_b$	$-5e_b$	$0e_b$	$5e_b$	$10e_b$	$15e_b$
	$-15e_b$	1.2814	.8410	.5499	.6532	1.0395	1.5047
		.6415	*.4541*	*.2952*	*.2332*	*.3287*	*.4982*
	$-10e_b$	1.2617	.7902	.4319	.5270	.9477	1.4312
		.6353	*.4431*	*.2744*	*.2012*	*.3033*	*.4795*
	$-5e_b$	1.2639	.7728	.3555	.4296	.8785	1.3742
		.6318	*.4359*	*.2589*	*.1736*	*.2820*	*.4640*
	$0e_b$	1.2880	.7910	.3491	.3834	.8374	1.3360
		.6311	*.4327*	*.2495*	*.1528*	*.2658*	*.4519*
	$5e_b$	1.3327	.8425	.4158	.4063	.8285	1.3181
		.6332	*.4336*	*.2471*	*.1419*	*.2556*	*.4436*
	$10e_b$	1.3961	.9217	.5287	.4887	.8529	1.3213
		.6380	*.4385*	*.2518*	*.1430*	*.2522*	*.4392*

Table 3. The standard derivation of pitch error [˚] according to the added gyroscope bias

Bias Error in Y-Axis		Bias Error in X-Axis: $-10e_b$	$-5e_b$	$0e_b$	$5e_b$	$10e_b$	$15e_b$
	$-15e_b$	1.2368	1.1447	1.0818	1.0533	1.0620	1.1069
		.3818	*.3696*	*.3624*	*.3606*	*.3642*	*.3730*
	$-10e_b$	.8694	.7551	.6811	.6611	.6995	.7878
		.2482	*.2319*	*.2235*	*.2238*	*.2328*	*.2494*
	$-5e_b$	.5776	.4261	.3303	.3405	.4495	.6060
		.1749	*.1553*	*.1473*	*.1527*	*.1701*	*.1962*
	$0e_b$	.5128	.3801	.3251	.3824	.5158	.6821
		.2296	*.2182*	*.2159*	*.2229*	*.2383*	*.2606*
	$5e_b$	.7374	.6774	.6735	.7265	.8255	.9562
		.3577	*.3525*	*.3531*	*.3595*	*.3713*	*.3880*
	$10e_b$	1.0846	1.0605	1.0737	1.1228	1.2034	1.3096
		.5063	*.5040*	*.5058*	*.5117*	*.5216*	*.5350*

DOI: http://dx.doi.org/10.5139/IJASS.2016.17.2.222

it is still excessive. In the contrast, the ΔVs measurement has very low noise (deltaV). Using the same sensor data, much improved measurement accuracy is achieved even without data pre-processing. The noise performances can be evaluated with the reference attitude from SPAN. Especially, in the high acceleration span at 5200 sec, the noise of all the reference methods is dramatically incising, but the ΔVs method can reduced this noise efficiently.

In Fig. 7, the Kalman Filter (KF) results with the measurements and gyroscope are shown. For the optimal results, each KFs are independently tuned, so each filters have the different tuning values. At 5200 sec in the figure, the reference methods show little unstable error results. But, during all span of experiment, all results have similar error performance. The reason is that these methods use same gyroscope, and the gyroscope has enough performance not to depend on the measurement so much for making the attitude result.

The previous estimation results are obtained assuming an accurate estimation on gyroscope bias during initial alignment periods. For practical application, a sensitivity analysis considering initial estimation error conditions is investigated.

In Fig. 8, the error results of the reference methods

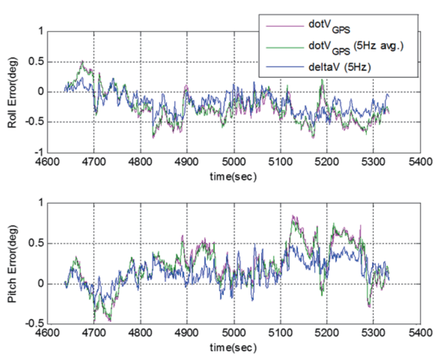

Fig.7. The attitude errors of the ΔVs method and reference methods

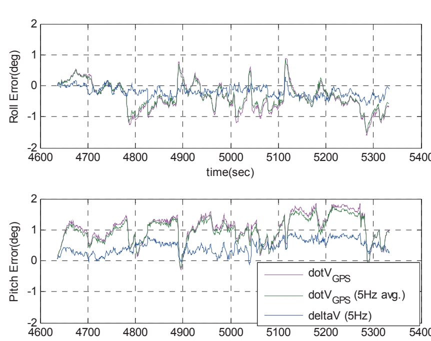

Fig.8. The result of the ΔVs method with respect to the reference result in bias environment

increased when the gyroscope bias error is added. In the figure, the added error is 10 times bigger value of the in-run bias stability (25°/hr) in the IMU specification. This bias is added at Y-axis, so the pitch error mainly occurs. For above results in Fig. 7, all filter tuning values are already set for the optimal results. So, at the reference methods, the results are depend on the gyroscope performance more, because of the high noise of the measurement. But, when the bias error is added, these things could be error sources. In the contrast, the ΔVs method have less error result, because of the low noise measurement performance.

Table 2 and 3 summarize the estimation results when an initial error is intentionally applied. Each tables show the roll and pitch error deviations from nominal condition with variations in initial estimate of gyro bias. The numbers in these tables means the standard variation of attitude results from SPAN. The horizontal index in the tables represents the applied estimation error from the true gyro bias in X-axis; the vertical index represents the applied estimation error in Y-axis.

The result of Fig. 8 is placed at the 3rd column of the bottom in these tables. The applied bias error increases or decreases by the 5 times step of 25°/hr (e_b) as the in-run bias stability specification of the employed gyroscope. In the these tables, the numbers in green color cells are the standard variation of the reference ARS result with GPS, and the numbers in blue cells are the standard variation of the proposed ΔVs method result. In any cases, ΔVs estimation errors of roll and pitch are more accurate than the traditional ARS estimation result. That means ΔVs method has more benefit comparing with the reference method in added bias.

Table 4 shows the computational time of the proposed method and other methods. 5Hz measurement update rate methods are faster than 100Hz methods. In this table, the ΔVs method is the 2nd fastest way comparing with other methods. According to this table, ΔVs method is reasonable enough to adjust real industry areas.

Table 4. The Computational Time

	Measurement Update Rate	Computational Time (100 Times Average)
Traditional ARS	100 Hz	9.4201 sec
$\dot{V}_{GPS}$ ARS	100 Hz	9.6768 sec
$\dot{V}_{GPS}$ ARS (5Hz Acc. Avg.)	5 Hz	2.7935 sec
ΔVs Integration (Multi-Window)	5 Hz	4.0610 sec

CPU: Intel® Core™ i5 CPU 750 2.66GHz
Data: About 700 sec, 100Hz IMU rate, 5Hz GPS rate

5. Conclusion

This paper newly proposes an efficient horizontal attitude estiamtion scheme, which is based on the suggested measurement formulation of the Kalman filter. With the assumption of slowly-varying sensor bias and weak acceleration, raw level sensor measurement is effectively processed with the numerical integration method to compute the velocity differential vector, ΔVs between IMU and GPS. The introduced method takes a quarternion based approach similar to the traditional ARS, yet a much better performance is achieved comparing with reference ARS methods. Since the proposed method directly computes the measurement of the Kalman filter during the integration period, the error convergence is very fast. Consequently, it can be easily applied to an integarted navigation system with a low cost IMU, GPS and microprocessor. Also it is expected future work of the method includes the extended estimation of the gyroscope bias and yaw angle for a full AHRS capacity.

Acknowledgement

This research was financially supported by the Korea Institute for Advancement of Technology(MOTIE, No.R0004086) and National Research Fund(NRF-2016R1A2B4010719).

References

[1] Hua, M. D., "Attitude estimation for accelerated vehicles using GPS/INS measurements", *Control Engineering Practice*, Vol. 18, Issue 7, July 2010, pp. 723-732.

[2] Martin, P. and Salaün, E., "Design and implementation of a low-cost observer-based attitude and heading reference system", *Control Engineering Practic*e, Vol. 18, Issue 7, July 2010, pp. 712–722.

[3] Martin, P. and Salaun, E., "The true role of accelerometer feedback in quadrotor control", *Proc. of IEEE International Conference on Robotics and Automation*, 2010.

[4] Pflimlin, J. M., Binetti, P., Soueres, P., Hamel, T. and Trouchet, D., "Modeling and attitude control analysis of a ducted-fan micro aerial vehicle", *Control Engineering Practice*, Vol. 14, 2006, pp. 1114–1120.

[5] Jiang, O., Zeng, Y., Liu, Q. and Jing, H., "Attitude and Heading Reference System for Quadrotor Based on MEMS Sensors", *2012 2nd IEEE International Conference on Instrumentation, Measurement, Computer, Communication and Control (IMCCC)*, Harbin, Chana, Dec. 2012.

[6] Sabatini, A. M., "Quaternion-Based Extended Kalman Filter for Determining Orientation by Inertial and Magnetic Sensing", *IEEE Transactions on Biomedical Engineering*, Vol. 53, No. 7, Jul. 2006.

[7] Tehrani, M. H., Garratt, M. A. and Anavatti, S., "Gyroscope Offset Estimation Using Panoramic Vision-Based Attitude Estimation and Extended Kalman Filter", *2012 2nd IEEE International Conference on Communications, Computing and Control Applications (CCCA)*, Marseilles, France, Dec. 2012.

[8] Madyastha, V. K., Ravindra, V. C., Vaitheeswaran, S. M. and Mallikarjunan, S., "A Novel INS/GPS Fusion Architecture for Aircraft Navigation", *2012 15th International Conference on Information Fusion (FUSION)*, Singapore, Jul. 2012.

[9] Skog, I., "A Low-Cost GPS Aided Inertial Navigation System for Vehicular Applications", Master's thesis, Royal Institute of Technology, Sweden, Mar. 2005, IR-SB-EX-0506.

[10] Schumacher, A., "Integration of a GPS aided Strapdown Inertial Navigation System for Land Vehicles", Master's thesis, Royal Institute of Technology, Sweden, Mar. 2006, XR-EE-SB 2006:006.

[11] Inman, D. J., *Engineering Vibrations*, 3rd Ed., Prentice Hall Inc., New Jersey, 2001.

[12] Titterton, D. H. and Weston, J. L., *Strapdown inertial navigation technology*, Peter Peregrinus Ltd., Stevenage, Herts, 1997.

[13] Bar-Itzhack, I. Y. and Oshman, Y., "Attitude determination from vector observations: Quaternion estimation", *IEEE Trans. Aerosp. Electron. Syst*, Vol. AES-21, No. 1, 1985, pp. 128–136.

[14] Chapra, S. C. and Canale, R. P., *Numerical Methods for Engineers*, 5th Ed. McGraw-Hill Companies Inc., New York, 2006.

[15] Grewal, M. S. and Andrews, A. P., *Kalman Filtering*, 3rd Ed. John Wiley and Sons Inc., New Jersey, 2008.

[16] Lewis, F. L, *Applied Optimal Control And Estimation*, Prentice Hall Inc., New Jersey, 1992.

[17] Ang, W. T., Khosla, P. and Riviere, C., "Kalman filtering for Real-Time Orientation Tracking of Handheld Microsurgical Instrument", *Proceedings of the IEEE International Conference on Intelligent Robots and Systems*, Vol. 3, 2004, pp. 2574-2580.

[18] Hoffman-Wellenhof, B., Lichtenegger, H. and Wasle, E., *GNSS – Global Navigation Satellite Systems*, Springer Wien NewYork, 2008.

[19] Metnia, N., Pflimlinb, J. M., Hamelc, T. and Souèresb, P., "Attitude and gyro bias estimation for a VTOL UAV", *Control Engineering Practice*, Vol. 14, 2006, pp. 1511–1520.

[20] Jurman, D., Jankovec, M., Kamnik, R. and Topic, M., "Calibration and data fusion solution for the miniature attitude and heading reference system", *Sensors and*

Actuators A: Physical, Vol. 138, No. 2, 2007, pp. 411-420.

[21] Romanovas, M., Klingbeil, L., Trachtler, M. and Manoli, Y., “Efficient orientation estimation algorithm for low cost inertial and magnetic sensor systems”, *IEEE/SP 15th Workshop on Statistical Signal Processing, SSP'09*, Cardiff, 2009, pp. 586-589.

[22] Sabatini, A. M., “Quaternion-based extended Kalman filter for determining orientation by inertial and magnetic sensing”, *IEEE Transactions on Biomedical Engineering*, Vol. 53, No. 7, 2006, pp. 1346-1356.

[23] Hemerly, E. M., Maciel, B. C., de P. Milhan, A. and Schad, V. R., “Attitude and heading reference system with acceleration compensation”, *Aircraft Engineering and Aerospace Technology*, Vol. 84, Issue 2, 2012, pp. 87-93.